IOP Conf. Series: Materials Science and Engineering **294** (2018) 012011 doi:10.1088/1757-899X/294/1/012011

The numerical modelling of mixing phenomena of nanofluids in passive micromixers

R Milotin and D Lelea

Politehnica University of Timisoara, Department for Mechanical Machines, Equipment and Transportation, B-dul Mihai Viteazu 1, 300223 Timisoara, Romania

E-mail: dorin.lelea@upt.ro

Abstract. The paper deals with the rapid mixing phenomena in micro-mixing devices with four tangential injections and converging tube, considering nanoparticles and water as the base fluid. Several parameters like Reynolds number (Re = 6 – 284) or fluid temperature are considered in order to optimize the process and obtain fundamental insight in mixing phenomena. The set of partial differential equations is considered based on conservation of momentum and species. Commercial package software Ansys-Fluent is used for solution of differential equations, based on a finite volume method. The results reveal that mixing index and mixing process is strongly dependent both on Reynolds number and heat flux. Moreover there is a certain Reynolds number when flow instabilities are generated that intensify the mixing process due to the tangential injections of the fluids.

1. Introduction

The micromixers are the good candidate for various applications in the engineering fields like bioreactors, drug-delivery devices or μ-TAS. The optimization of the channels configuration is the important task, in order to obtain the compactness, uniform concentration and temperature of the mixture and short mixing length. For passive mixing this might be obtained by magnifying the area of the fluids that come in contact, inducing instabilities or increasing the mixing path. Besides the micromixers could realize more rapid and dynamic chemical reactions. Special attention should be taken in effective mixing in low Re regime because high shear rates and some biological species are not compatible [1].

There is a large number of research papers on passive mixing in microchannels, both numerical and experimental, reported by various authors in last decade. Four different microfluidic configurations were analyzed by Jeon and Shin [2] numerically and the conclusion was that the best mixing efficiency at low Re has zig-zag. The results were also confirmed experimentally. The influence of the stream position was analyzed by Ansari et al. [3] regarding mixing phenomena in T-shape microchannels. It was found that stream position has more influence at low Re. Miranda et al. [4] investigated numerical analysis on a microfluidic device that has obstacles and a flow that alternates. Besides, the Σ-micromixer was analyzed and optimized by Tafti et al. [5]. The optimization of the micromixer with convergent-divergent sinusoidal walls taking into account both the pressure drop and the mixing efficiency was made by Afzal and Kim [6]. The optimization was made for Re of 30. The analysis showed a great variation in the ratio of throat width to depth of the convergent-divergent areas, whereas the quantitative relation of amplitude to wavelength of the sinusoidal walls maintained a mainly constant value. The microfluidic device for nano-drug delivery was numerically

explored by Kleinstreuer et al. [7]. The conclusion was that a better mixing efficiency of nanoparticles and a shorter mixing length than a simple T-shape configuration has a micromixer with baffles and injection unit. Lin and Yang [8] examined numerically the main issues on chaotic mixing. The mixing phenomena in T-type micromixer strengthened by J-shaped baffles was analyzed numerically and experimentally by Lin et al. [9]. They discovered that amount of mixing is raising as the number of baffles and Re raises. Long et al. [10] studied the numerical and experimental exploration of rapid vortex micromixers. Enhanced mixing is because of the bigger interfacial contact area and fluid convection. Review analysis on passive micromixers was published by Hardt et al [11] for μ-TAS and microreactors, Mansur et al. [12] and Kumar et al. [13]. SAR μ-reactor was analyzed by Fang and Yang [14] and Broboana et al. [15] studied unsteady diffusion process in Y- shaped micromixers. Lin et al. [16] explored quick circular micromixer with unbalanced driving force. The conclusion was that rotational flow was established even at Re = 2. Numerically planar configuration of passive micromixers with circular chambers was studied by Alam and Kim [17]. They tested four different configurations with Re = 0.1 – 100. They noticed that mixing performance is mainly dependent on micromixer configuration and Re. The micromixer they proposed has gorgeons mixing abilities at low Re but a poor behaviour at Re > 50. Dykman and Klebetsov [18] presented the review on gold nanoparticles in therapeutic and diagnosis applications.

In this paper the mixing efficiency is evaluated for nanofluid mixing in microneedle arrays.

2. Numerical details

The passive mixing phenomena was analyzed, considering the micromixer presented in Figure 1a based on the microneedle arrays [19] (Figure 1b). The geometry and the flow conditions are presented table 1. In the case of the microchannels conventional theories are appropriate to microtubes with diameters down to 100 μm accordingly to Lelea et al. [20].

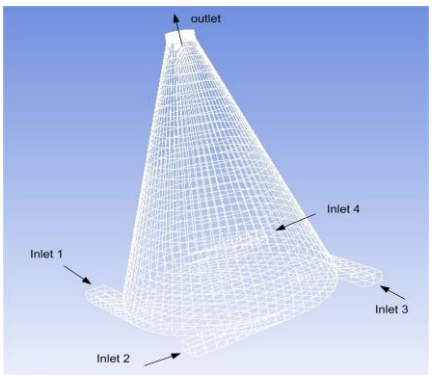

Figure 1a. The micromixer configuration

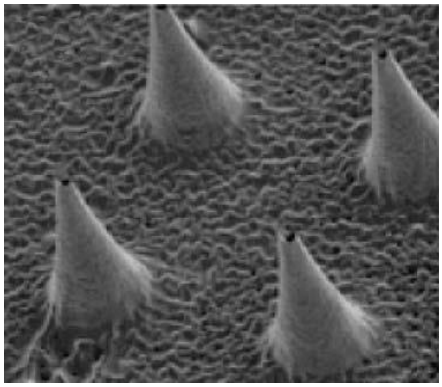

Figure 1b. The microneedle arrays [20]

Table 1. The geometry and fluid flow conditions

L, cm	*a, μm*	*b, μm*	D_{base}, *μm*
1	80	40	800
D_{out}, *μm*	$t_{out,}$ °C	*m*, kg/s	Re
100	37	$10^{-7} – 5\ 10^{-6}$	6.24 - 284

So the set of the Navier-Stokes equations can be used to analyze the present phenomena, as follows:

The conservation of mass

$$\frac{\partial(\rho \cdot u_i)}{\partial x_i} = 0 \tag{1}$$

The conservation of momentum

$$\frac{\partial(u_i \cdot \rho \cdot u_j)}{\partial x_i} = -\frac{\partial p}{\partial x_j} + \frac{\partial}{\partial x_i}\left(\mu \frac{\partial u_j}{\partial x_i}\right) \tag{2}$$

The conservation of species

$$\frac{\partial(u_i \cdot C)}{\partial x_i} = \frac{\partial}{\partial x_i}\left(D \frac{\partial C}{\partial x_i}\right) \tag{3}$$

The upcoming boundary conditions are determined for the micromixers presented in this paper:

- The fluid flow is stationary, incompressible and laminar;
- The fluid properties of the nanofluid and water were found as temperature dependent with the upcoming equations:

Thermophysical properties of the water:

Dynamic viscosity:

$$\mu(t) = 2.6412018 \cdot 10^{-4} + 0.0014009 \cdot e^{-\frac{t}{31.0578605}} \tag{4}$$

Density:

$$\rho(t) = 1000.0 \cdot \left(1 - \frac{t + 288.9414}{508929.2 \cdot (t + 68.12963) \cdot (t - 3.9863)^2}\right) \tag{5}$$

Thermal conductivity:

$$k(t) = -0.58166 + 6.355 \cdot 10^{-3} \cdot T - 7.964 \cdot 10^{-6} \cdot T^2 \tag{6}$$

Specific heat:

$$c_p(t) = 8958.9 - 40535 \cdot T + 0.11243 \cdot T^2 - 1.014 \cdot 10^{-4} \cdot T^3 \tag{7}$$

Thermophysical properties of nanofluid:

The nanofluid effective thermal conductivity normalized with the based fluid thermal conductivity is given as [21]:

$$\frac{k_{eff}}{k_{bf}} = 1 + 64.7 \cdot \phi^{0.7460} \left(\frac{D_{bf}}{D_p}\right)^{0.3690} \cdot \left(\frac{k_p}{k_{bf}}\right)^{0.7476} \cdot \mathrm{Pr}^{0.9955} \cdot \mathrm{Re}^{1.2321} \tag{8}$$

The Pr is defined as:

$$\mathrm{Pr} = \frac{\mu}{\rho_{bf} \cdot \alpha} \tag{9}$$

The Re is calculated as:

$$\mathrm{Re} = \frac{\rho_{bf} \cdot k_b \cdot T}{3 \cdot \pi \cdot \mu^2 \cdot l_{bf}} \tag{10}$$

where k_b = 1.3807x10^{-23} J/K, l_{bf} = 0.17 nm and D_{bf} = 0.384 nm.

The temperature dependent viscosity of water is defined with equation (4).

The effective density is defined as:

$$\rho_{eff} = (1-\phi) \cdot \rho_f + \phi \cdot \rho_p \tag{13}$$

The effective specific heat is calculated as:

$$c_{peff} = \frac{(1-\phi) \cdot (\rho \cdot c_p)_f + \phi \cdot (\rho \cdot c_p)_p}{\rho_{eff}} \tag{14}$$

The effective viscosity is a sum of base fluid viscosity and apparent viscosity:

$$\mu_{eff} = \mu_{bf} + \mu_{app} \tag{15}$$

The base fluid viscosity (water) is calculated by the equation (4), while the evident viscosity of the nanofluid is explained by the upcoming relation [22]:

$$\mu_{app} = \frac{\rho_p \cdot V_b \cdot d_p^2}{72 \cdot C \cdot \delta} \tag{16}$$

where the Brownian velocity is defined as:

$$V_b = \frac{1}{d_p} \sqrt{\frac{18 \cdot K_b \cdot T}{\pi \cdot \rho_p \cdot d_p}} \tag{17}$$

A distance between the centers of the particles is obtained from:

$$\delta = \sqrt[3]{\frac{\pi}{6 \cdot \phi}} \cdot d_p \tag{18}$$

The correction factor is defined as:

$$C = \mu_{bf}^{-1} \cdot \left[(c_1 \cdot d_p + c_2) \cdot \phi + (c_3 \cdot d_p + c_4) \right] \tag{19}$$

where: c_1 = -1.2331·10^3, c_2 = -1.5331·10^{-6}, c_3 = 94.383 and c_4 = -4.5731·10^{-7}

- The properties of the gold particles are defined as: ρ_p = 19300 kg/m^3, c_{pp} = 1290 J/kg K, k_p = 314 W/mK.
- Because of the low flow rates, the viscous dissipation is neglected;
- The uniform velocity field and the constant temperature are imposed at the channel inlet, while at the outlet the partial derivatives of the velocity and temperature in the streamwise direction are vanishing;

The nanofluid was considered as Fluid 1 and water as Fluid 2, with inlet cross-sections presented in Figure 1a. Mass fraction is considered 1 at the nanofluid and 0 for water inlets.

The set of the partial differential equations with boundary conditions are solved using the Ansys Fluent commercial solver [23] with methods described in [24]. The Simple algorithm is used for the velocity-pressure coupling solution and QUICK scheme for discretization of the partial differential equations for momentum and concentration species. The under-relaxation factors are used for pressure field (α = 0.3), momentum conservation (α = 0.5) and species conservation (α = 0.8). The convergence criterion is defined as:

$$R^{\phi} = \frac{\sum_{cells,P} \left| \sum_{nb} a_{nb} \cdot \phi_{nb} + b - a_p \phi_p \right|}{\sum_{cells,P} \left| a_p \phi_p \right|} \tag{20}$$

The residuals for velocity components, continuity equation and concentration field were 10^{-8}.

3. Results and discussion

The mixing behavior of micromixer with four tangential inlets was evaluated in terms of mixing index defined with the following equation:

$$M = 1 - \sqrt{\frac{\sigma^2}{\sigma_{max}^2}} \tag{21}$$

where the standard deviation of the mass fraction was calculated at specific cross-sections with the following relation:

$$\sigma = \sqrt{\frac{\sum_{i=1}^{n}(c_i - c_{av})^2}{n}} \tag{22}$$

the c_{av} is the average of the mass fraction c_i at specific cross-section defined with the following relation:

$$c_{av} = \frac{\sum_{i=1}^{n} c_i}{n} \tag{23}$$

Besides, Re is calculated with the following relation:

$$\mathrm{Re} = \frac{\rho \cdot u_{av} \cdot D_i}{\mu} \tag{24}$$

The temperature dependent diffusion coefficient is defined as:

$$D = \frac{k_b \cdot T}{6 \cdot \pi \cdot \mu \cdot d_p} \tag{25}$$

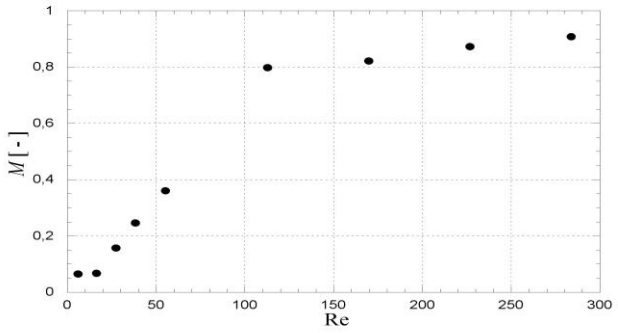

Figure 2. The mixing index versus Re

In Figure 2 the mixing versus Re is presented. It is observed that mixing index is very low for low values of Re < 20. There are two main reasons for this behaviour. The first one is the outcome of low diffusion coefficient $D = 10^{-11}$. The second one is related to stable hydrodynamic field without the swirl motion generated by tangential inlets. Besides the molecular diffusion is the main mixing mechanism in this case. As the Re increases the fluid flow became unstable and the swirl motion is initiated inside the micromixer. The outcome might be observed in the rapid increasing of the mixing index. This mixing behavior is observed for 30 < Re < 113. For Re > 113 the mixing index is slightly increasing from $M = 0.8 – 0.9$.

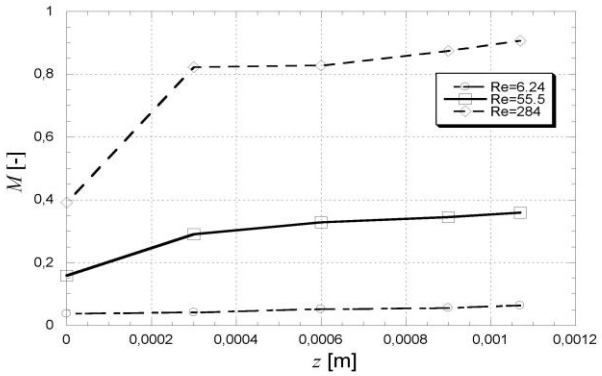

Figure 3. The axial distribution of the mixing index

In Figure 3 local distribution of the mixing index is presented for three different Re. In the case of very low Re = 6.24 the mixing index is almost constant regardless the axial position $M < 0.1$. For Re = 55.5 the mixing index slightly increases from $M = 0.2$ to $M = 0.3$ immediately after the inlet cross-sections remaining almost constant for the rest of the micromixer. This behavior indicated that the swirl motion could not be supported due to the hydrodynamic losses.

In the case of higher Re = 284, the mixing index sharply increases from M = 0.4 to M = 0.8, in the first quarter of the micromixer. For the rest of the axial distance the mixing index slightly increases to M = 0.9. In this case the swirl motion generated by four tangential inlets is fully established so the advection is responsible for better nanofluid mixing.

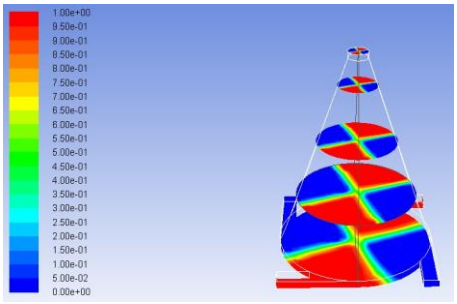

Figure 4. The mass fraction of nanofluids for Re = 6.24

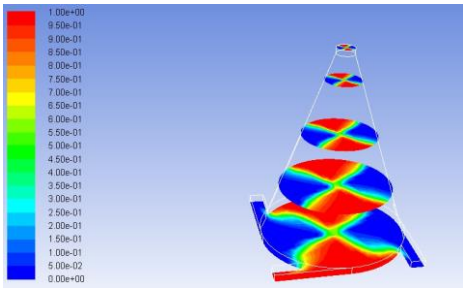

Figure 5. The mass fraction of nanofluids for Re = 27.5

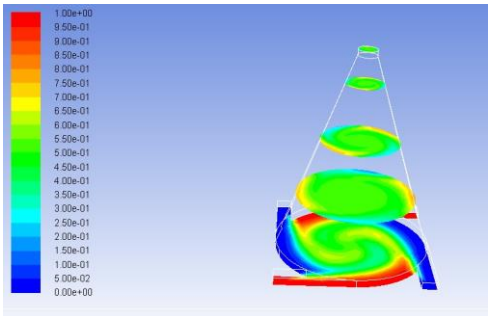

Figure 6. The mass fraction of nanofluids for Re = 170

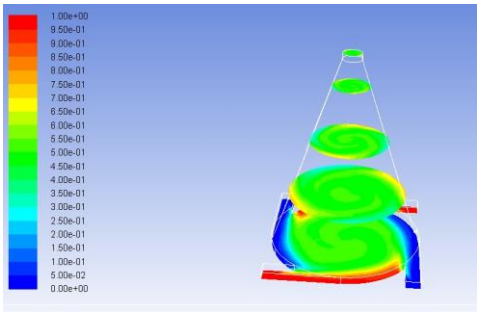

Figure 7. The mass fraction of nanofluids for Re = 284

In Figure 4 – 5 the nanofluid mass fraction plot for Re = 6.24 and 27.5 is presented at different axial positions. It might be observed that for Re = 6.24 the mass fraction field is almost unchanged regardless the axial position. As Re = 27.5, the minor flow instabilities are observed only near the inlet cross-sections.

As the Re increases to Re = 170 (Figure 6), the swirl motion is fully established and the nanofluid mixing is almost completely done up to the outlet cross-section. The same conclusion might be outlined for Re = 284 (Figure 7).

4. Conclusions

The analysis regarding the mixing efficiency of the micromixer with four tangential inlets and converging microchannel, designed for nano-drug delivery was made. The following conclusions are outlined:

- The hydrodynamic conditions strongly influence the mixing efficiency.
- The four inlet jets enlarged the contact area and at higher Re create the swirl flow that was a result in better mixing.
- The real diffusion coefficient, based on temperature, influence the passive mixing phenomena.
- The rapid mixing influenced by advection is established for $55 < Re < 100$.
- The better mixing behavior is limited by the body temperature ($t = 37\ ^oC$)
- Moreover the higher mixing index might be obtain by increasing the length of the outlet channel.

References

[1] Nguyen N T 2008 *Micromixers-Fundamentals, Design and Fabrication,* William Andrew
[2] Jeon W and Shin C B 2009 Design and simulation of passive mixing in microfluidic systems with geometric variations, *Chem. Eng. J.* **152** 575-582
[3] Ansari M A, Kim K Y and Kim S M 2010 Numerical study of the effect on mixing of the position of fluid stream interfaces in a rectangular microchannel, *Microsyst Technol* **16** 1757–1763
[4] Miranda J M, Oliveira H, Teixeira J A, Vicente A A, Correia J H and Minas G 2010 Numerical study of micromixing combining alternate flow and obstacles, *Int Commun Heat Mass* **37** 581–586
[5] Tafti E Y, Kumar R and Cho H J 2011 Diffusive mixing through velocity profile variation in microchannels, *Exp Fluids* **50** 535–545
[6] Afzal A and Kim K Y 2014 Multi-Objective Optimization of a Micromixer with Convergent-Divergent Sinusoidal Walls, *Chem Eng Commun* **202**(10) 1324-1334
[7] Kleinstreuer C, Li J and Koo J 2008 Microfluidics of nano-drug delivery, *Int J Heat Mass Tran* **51** 5590–5597
[8] Lin K W and Yang J T 2007 Chaotic mixing of fluids in a planar serpentine channel, *Int J Heat Mass Tran* **50** 1269–1277
[9] Lin Y C, Chung Y C and Wu C Y 2007 Mixing enhancement of the passive microfluidic mixe with J-shaped baffles in the tee channel, *Biomed Microdevices* **9** 215–221
[10] Long M, Sprague M A, Grimes A A, Rich B D and Khine M 2009 A simple three-dimensional vortex micromixer, *Appl Phys Lett* **94** 133501
[11] Hardt S, Drese K S, Hessel V and Schonfeld F 2005 Passive micromixers for applications in the microreactor and μ-TAS fields, *Microfluid Nanofluid* **1** 108-118
[12] Mansur E A, Mingxing Y E, Yundong W and Youyuan D 2008 A State-of-the-Art Review of Mixing in Microfluidic Mixers, *Chinese J Chem Eng* **16**(4) 503-516
[13] Kumar V, Paraschivoiu M and Nigam K D P 2011 Single-phase fluid flow and mixing in microchannels, *Chem Eng Sci* **66** 1329-1373
[14] Fang W F and Yang J T 2009 A novel microreactor with 3D rotating flow to boost fluid reaction and mixing of viscous fluids, *Sensor Actuat B-Chem* **140** 629-642

[15] Broboana D, Balan C M, Wohland T and Balan C 2011 Investigations of the unsteady diffusion process in microchannels, *Chem Eng Sci* **66** 1962-1972
[16] Lin C H, Tsai C H, Pan C W and Fu L M 2007 Rapid circular microfluidic mixer utilizing unbalanced driving force, *Biomed Microdevices* **9** 43-50
[17] Alam A and Kim K Y 2013 Mixing performance of a planar micromixer with circular chambers and crossing constriction channels, *Sensor Actuat B-Chem* **176** 639-652
[18] Dykman L A and Khlebetsov N G 2011 Gold Nanoparticles in Biology and Medicine: Recent Advances and Prospects, *Reviews – Acta Naturae* **3**(2) 34-55
[19] Wang W and Soper S 2007 *Bio-Mems: Technologies and Applications*, CRC Press, New York
[20] Lelea D, Nishio S and Takano K 2004 The experimental research on microtube heat transfe and fluid flow of distilled water, *Int J Heat Mass Tran* **47** 2817-2830
[21] Chon C H, Kihm K D, Lee S P and Choi S U S 2005 Empirical correlation finding the role of temperature and particle size for nanofluid (Al_2O_3) thermal conductivity enhancement, *Applied Physics Letters* **87** 153107-(1-3)
[22] Masoumi N, Sohrabi N and Behzadmehr A 2009 A new model for calculating the effective viscosity of nanofluids, *J. Phys. D: Appl. Phys* **42** 055501-(1-6)
[23] ***2011 *Ansys Fluent* 14.0 documentation, Ansys Inc.
[24] Patankar S V 1980 *Numerical Heat Transfer and Fluid Flow*, McGraw Hill, New York